Research Square

Preprints are preliminary reports that have not undergone peer review.
They should not be considered conclusive, used to inform clinical practice,
or referenced by the media as validated information.

Growth differentiation factor 15 is associated with diabetic kidney disease severity and attenuates ferroptosis-related injury and inflammation in renal tubular epithelial cells

Xiaomeng Zhang
Hebei North University
Huihui Bai
North China University of Science and Technology
Kehan Zhao
Hebei North University
Zhiqi Wang
Hebei North University
Junheng Ding
North China University of Science and Technology
Xingyue Ye
Hebei Medical University
Jiale Niu
Hebei General Hospital
Yamin Lu
xyluyamin@163.com

Hebei General Hospital

Article

Keywords: diabetic kidney disease, GDF15, ferroptosis, renal tubular epithelial cells, inflammation

Posted Date: November 13th, 2026

DOI: https://doi.org/10.21203/rs.3.rs-11522846/v1

License: This work is licensed under a Creative Commons Attribution 4.0 International License.
Read Full License

Additional Declarations: No competing interests reported.

Growth differentiation factor 15 is associated with diabetic kidney disease severity and attenuates ferroptosis-related injury and inflammation in renal tubular epithelial cells

Xiaomeng Zhang[1,4], Huihui Bai[2,4], Kehan Zhao[1,4], Zhiqi Wang[1,4], Junheng Ding[2,4], Xingyue Ye[3], Jiale Niu[5], Yamin Lu[4*]

[1]Graduate School, Hebei North University, Zhangjiakou, Hebei 075000, P.R. China

[2]Graduate School, North China University of Science and Technology, Tangshan, Hebei 063210, P.R. China

[3]College of Basic Medicine, Hebei Medical University, Shijiazhuang, Hebei 050017, P.R. China

[4]Department of Clinical Laboratory, Hebei General Hospital, Hebei Key Laboratory of Molecular Medicine, Hebei Clinical Research Center for Medical Laboratory, Shijiazhuang, Hebei 050051, P.R. China

[5]Department of Blood Transfusion, Hebei General Hospital, Hebei Key Laboratory of Molecular Medicine, Hebei Clinical Research Center for Medical Laboratory, Shijiazhuang, Hebei 050051, P.R. China.

Correspondence to:

Yamin Lu , Department of Clinical Laboratory, Hebei General Hospital; Hebei Key Laboratory of Molecular Medicine; Hebei Clinical Research Center for Medical Laboratory Medicine, Shijiazhuang 050051, Hebei, China.E-mail: xyluyamin@163.com

Abstract

Background. Ferroptosis and inflammation contribute to renal tubular injury in diabetic kidney disease (DKD), but the clinical significance and biological role of growth differentiation factor 15

(GDF15) remain unclear. We investigated the association between circulating GDF15 and DKD severity and explored the potential role of GDF15 in modulating glucolipotoxic injury in renal tubular epithelial cells.

Methods. This clinical study included 43 healthy controls, 40 patients with type 2 diabetes mellitus (T2DM) without DKD and 38 patients with DKD. Serum GDF15, iron-metabolism parameters, ferroptosis-related antioxidant markers and inflammatory cytokines were assessed. HK-2 cells were exposed to high glucose plus palmitic acid (HGPA) and treated with ferrostatin-1 (Fer-1) or subjected to GDF15 knockdown or overexpression. Cell viability, reactive oxygen species, malondialdehyde, glutathione, Fe^{2+} and molecular markers of ferroptosis, iron metabolism and inflammation were evaluated.

Results. Circulating GDF15 levels were higher in patients with DKD and were associated with albuminuria, renal function indices, altered iron-related parameters, reduced circulating GPX4 and GSH levels, and inflammatory markers. In HK-2 cells, high glucose combined with palmitic acid (HGPA) increased ROS, MDA, and Fe^{2+} levels, decreased GSH, downregulated GPX4 and SLC7A11, and increased ACSL4 expression. These changes were accompanied by increased GDF15 expression and NF-κB-associated inflammatory responses. GDF15 knockdown exacerbated these HGPA-associated alterations, whereas GDF15 overexpression attenuated them. Fer-1 partially alleviated the changes associated with GDF15 knockdown, supporting the involvement of ferroptosis-related processes in the observed cellular injury.

Conclusions. Elevated circulating GDF15 was associated with DKD severity and renal injury, while cellular experiments suggested a protective role of GDF15 under glucolipotoxic stress. The observed effects involved ferroptosis-associated oxidative injury, iron-metabolism-related changes, and

inflammatory signaling. Further studies are needed to establish the underlying pathways and determine the clinical utility of GDF15 in DKD.

Keywords: diabetic kidney disease; GDF15; ferroptosis; renal tubular epithelial cells; inflammation

Highlights:

Circulating GDF15 is associated with DKD severity and renal injury.

GDF15 modulates ferroptosis-associated injury in HGPA-treated HK-2 cells.

GDF15 modulation is accompanied by changes in iron-related genes and NF-κB-associated inflammatory signaling.

Introduction

Among the microvascular complications of diabetes, diabetic kidney disease (DKD) is one of the most prevalent and is a major driver of chronic kidney disease progression to end-stage kidney disease [1]. Traditional research has focused primarily on glomerular injury [2]; however, accumulating evidence indicates that tubulointerstitial injury is closely associated with renal function decline and adverse renal outcomes in patients with DKD [3]. Proximal tubular epithelial cells have high energy demands and, under diabetic conditions, are continuously exposed to hyperglycemia, lipid overload, oxidative stress, and inflammation, making them important targets of diabetic metabolic injury. Therefore, elucidating the regulatory mechanisms underlying tubular epithelial cell injury under glucolipotoxic conditions may provide new insights into DKD risk stratification and therapeutic intervention.

Ferroptosis is a regulated form of cell death driven by iron-dependent membrane phospholipid peroxidation and characterized by impaired glutathione peroxidase 4 (GPX4) activity and lipid peroxide accumulation. Hallmark features include intracellular accumulation of redox-active iron, glutathione (GSH) depletion, impaired GPX4-dependent antioxidant defense, and enhanced lipid

peroxidation [4]. Reduced GPX4 and SLC7A11 expression, increased iron burden, and lipid peroxide accumulation have been observed in renal tissues from patients with diabetes, diabetic animal models, and high-glucose-treated tubular epithelial cells, whereas ferroptosis inhibitors such as Ferrostatin-1 (Fer-1) can alleviate tubular injury [5, 6]. Moreover, db/db mice and HK-2 cells exposed to high glucose and lipid overload exhibit prominent ferroptotic features, suggesting that glucolipid metabolic disturbances may promote DKD progression by disrupting antioxidant defenses and iron homeostasis [7, 8]. Iron-dependent oxidative stress may also activate inflammatory pathways such as NF-κB, whereas inflammation can in turn alter iron metabolism and antioxidant capacity. Thus, ferroptosis, iron-homeostasis disturbance, and inflammation may jointly shape the pathological microenvironment of diabetic tubular injury.

Growth differentiation factor 15 (GDF15) is a stress-responsive cytokine whose expression increases in response to oxidative stress, mitochondrial dysfunction, metabolic disturbance, and tissue injury. Previous studies have shown that circulating or urinary GDF15 levels are associated with DKD, reduced estimated glomerular filtration rate (eGFR), and adverse renal outcomes [9-11]. However, elevated GDF15 does not necessarily imply a direct pathogenic role; it may reflect tissue injury and renal function decline or represent a compensatory protective response. Experimental studies have shown that genetic deletion of GDF15 aggravates tubular and interstitial injury in mouse models of both type 1 and type 2 diabetes [12], although ferroptosis-related markers were not assessed. Conversely, GDF15 overexpression or exogenous supplementation can attenuate diabetic renal injury and suppress AGE/RAGE- and TLR4/MyD88/NF-κB-related inflammatory signaling [13]. GDF15 has also been reported to preserve Klotho expression and limit NF-κB activation in other models of kidney injury [14] and to inhibit ferroptosis by strengthening antioxidant defenses [15]. Nevertheless, whether GDF15 directly regulates glucolipotoxicity-induced ferroptosis in renal

tubular epithelial cells, and how this process relates to iron-metabolism disturbance and NF-κB-associated inflammation, remain unclear.

Against this background, we first examined circulating GDF15 in relation to renal indices, ferroptosis-related antioxidant markers, iron-metabolism parameters, and inflammatory mediators in healthy controls and patients with T2DM with or without DKD. We then used an HGPA-treated HK-2 cell model, together with GDF15 knockdown, GDF15 overexpression, and Fer-1 treatment, to investigate whether GDF15 modulates glucolipotoxic injury. This combined approach was intended to place the clinical associations in a functional cellular context and to explore the involvement of ferroptosis-associated oxidative stress, iron-related transcriptional changes, and NF-κB-associated inflammatory responses.

Materials and Methods

Main reagents

HK-2 cells were obtained from the China Center for Type Culture Collection (CCTCC; GDC0152). Fetal bovine serum (FBS) was purchased from ScienCell Research Laboratories (USA; cat. no. 0500). Ferrostatin-1 (Fer-1; Cayman Chemical, cat. no. 17729), dimethyl sulfoxide (DMSO; Solarbio, cat. no. D8371), penicillin-streptomycin-glutamine supplement (Gibco, A58736-1), and Lipofectamine 2000 (Thermo Fisher Scientific) were used. Assay kits for malondialdehyde (MDA; Yakeyin, cat. no. KTB1050), glutathione (GSH; Yakeyin, cat. no. KTB1600), ferrous iron (Fe^{2+}; Yakeyin, cat. no. KTB1116), and reactive oxygen species (ROS; Yakeyin, cat. no. KTB1910) were used according to the manufacturers' instructions. Horseradish peroxidase (HRP)-conjugated goat anti-rabbit IgG secondary antibodies and all primary antibodies were obtained from Zhengneng Biotechnology, including antibodies against GDF15 (R24424), GPX4 (R381958), SLC7A11 (R382036), ACSL4 (R24265), NF-κB p65 (R25149), and phosphorylated NF-κB p65 (p-NF-κB p65;

310013). Reagents for RNA extraction, cDNA synthesis, and quantitative real-time PCR (qRT-PCR) were purchased from TIANGEN Biotech, and primers were synthesized by Tsingke Biotechnology. GDF15 siRNAs and the negative-control siRNA (siNC) were purchased from NEORABIO, and the GDF15 overexpression plasmid was obtained from Yubao Biotechnology. All ELISA kits were supplied by Jiangsu Meimian Industrial Co., Ltd.

Study design and participants

This study combined a clinical cross-sectional investigation with in vitro mechanistic experiments. The clinical component was approved by the Ethics Committee of Hebei General Hospital, and all participants provided informed consent. A total of 78 patients with T2DM treated at Hebei General Hospital together with 43 healthy individuals undergoing routine physical examination as the normal control (NC) group. According to renal function and urinary albumin levels, patients with T2DM were classified into a T2DM without DKD group (n=40) and a DKD group (n=38).

T2DM was diagnosed on the basis of a fasting plasma glucose level ≥7.0 mmol/L, a 2-h plasma glucose level ≥11.1 mmol/L during an oral glucose tolerance test, or a random plasma glucose level ≥11.1 mmol/L in the presence of typical hyperglycemic symptoms; in participants without typical symptoms, repeat testing was required for confirmation. The T2DM group was defined by a urinary albumin-to-creatinine ratio (UACR) <30 mg/g and an eGFR ≥60 mL/min/1.73 m^2, with other renal diseases excluded. DKD was defined as established T2DM with UACR ≥30 mg/g and/or eGFR <60 mL/min/1.73 m^2 after exclusion of other primary or secondary kidney diseases. Participants in the NC group had no history of diabetes or kidney disease, normal glucose and hepatic/renal function, UACR <30 mg/g, and eGFR ≥60 mL/min/1.73 m^2.

Exclusion criteria were as follows: (1) type 1 diabetes, gestational diabetes, or other specific

types of diabetes; (2) acute kidney injury, primary kidney disease, or urinary tract infection; (3) acute infection, infectious disease, or autoimmune disease; (4) severe cardiovascular, hepatic, respiratory, neurological, or psychiatric disease; (5) malignancy or recent radiotherapy/chemotherapy; (6) pregnancy or lactation; and (7) incomplete clinical data or biological samples.

Measurement of serum biomarkers

Peripheral venous blood was collected from each participant, and serum was separated and stored until analysis. Serum GDF15, GPX4, GSH, IL-1β, IL-17, IL-10, and IL-6 levels were measured using enzyme-linked immunosorbent assay (ELISA) kits. All procedures were performed strictly according to the manufacturers' instructions.

Cell culture and treatments

HK-2 cells were cultured in DMEM supplemented with 10% FBS, 1% L-glutamine supplement, and 1% penicillin-streptomycin (final concentrations, 100 U/mL and 100 μg/mL, respectively) at 37°C in a humidified atmosphere containing 5% CO_2. Cells were used for subsequent experiments at approximately 70-80% confluence.Palmitic acid (PA) was prepared using a BSA-conjugation method. PA was dissolved in 0.1 mol/L NaOH to generate a 100 mmol/L sodium palmitate intermediate solution, which was then slowly added to prewarmed 10% fatty-acid-free BSA and incubated with shaking at 55°C for 30 min to obtain a 5 mmol/L PA-BSA stock solution. The solution was sterilized through a 0.22-μm filter before use. The normal-glucose (NG) group was cultured in DMEM containing 5.5 mmol/L glucose. The high-glucose plus palmitic acid (HGPA) group was treated with 30 mmol/L glucose and 0.2 mmol/L PA for 24 h. For the HGPA+Fer-1 group, cells were pretreated with 1 μmol/L Fer-1 for 2 h and then co-treated with HGPA for 24 h. The NG group received an equivalent amount of BSA vehicle, and the final DMSO concentration was kept identical across groups.

CCK-8 cell viability assay

HK-2 cells were adjusted to 5.0×10^4 cells/mL and seeded into 96-well plates at 100 μL per well. Following attachment, cells were exposed to the indicated treatments for 24 or 48 h. At each endpoint, 10 μL of CCK-8 solution was added to each well, followed by incubation at 37°C for 2 h. Absorbance at 450 nm (A450) was measured using a microplate reader to assess cell viability. Cell viability (%) was calculated as (Aexperimental − Ablank)/(Acontrol − Ablank) ×100%.

Cell transfection

HK-2 cells were seeded in 6-well plates and transfected at approximately 70-80% confluence using Lipofectamine 2000. siGDF15, siNC, the GDF15 overexpression plasmid, or the empty vector was separately mixed with Opti-MEM. Lipofectamine 2000 was diluted in Opti-MEM and incubated for 5 min at room temperature. The two solutions were then combined and incubated for 20 min at room temperature before being added dropwise to antibiotic-free medium. The medium was replaced with complete medium 6 h after transfection. At 24 h after transfection, cells were pretreated with 1 μmol/L Fer-1 for 2 h and subsequently exposed to HGPA for 24 h. GDF15 knockdown or overexpression efficiency was verified by qRT-PCR and Western blotting. To identify the most effective GDF15-targeting sequence, HK-2 cells were transfected with siNC or one of three different siGDF15 sequences. After 24 h of transfection, cells were exposed to HGPA for an additional 24 h, and GDF15 expression was assessed by qRT-PCR and Western blotting. The siRNA producing the greatest knockdown was selected for subsequent experiments (Supplementary Table 1).

GSH assay

GSH was measured according to the manufacturer's protocol. Approximately 5×10^6 cells from each group were collected, washed with ice-cold PBS, and centrifuged at 800×g for 2 min. One milliliter of extraction buffer was added, and cells were sonicated on ice for 5 min. After

centrifugation for 10 min, the supernatant was collected. Blank, standard, and sample wells were prepared and incubated for 2 min at room temperature in the dark. Absorbance was measured at 412 nm, and GSH content was calculated from the standard curve.

MDA assay

MDA was measured according to the manufacturer's protocol. Approximately 1×10^7 cells from each group were collected, washed with ice-cold PBS, and lysed in 0.5 mL extraction buffer on ice for 5-10 min. Lysates were centrifuged at 13,000×g for 10 min at 4°C. A 100-μL aliquot of supernatant was mixed with 300 μL reaction solution and incubated at 95°C for 30 min. After cooling on ice, samples were centrifuged at 10,000×g for 10 min. A 200-μL aliquot of the supernatant was used to measure absorbance at 532 and 600 nm, and MDA content was calculated according to the manufacturer's instructions.

Measurement of Fe^{2+} content

Fe^{2+} content was determined according to the manufacturer's protocol. Approximately 1×10^7 cells from each group were collected, washed with ice-cold PBS, and lysed in 0.5 mL extraction buffer on ice for 10 min, with gentle inversion every 2 min. Blank, standard, and sample tubes were prepared. A 200-μL aliquot of supernatant was mixed with 100 μL reagent I and incubated at 37°C for 10 min. Subsequently, 100 μL chloroform was added, samples were vortexed for 2 min, and centrifuged at 10,000×g for 5 min. Two hundred microliters of the upper aqueous phase was transferred to a 96-well plate, absorbance was measured at 593 nm, and Fe^{2+} content was calculated from the standard curve.

Measurement of intracellular ROS

Intracellular ROS levels in HK-2 cells were measured using DCFH-DA. Cells were incubated

with 10 μM DCFH-DA at 37°C for 30 min in the dark, washed 1-2 times, and fluorescence intensity was quantified using a multimode fluorescence microplate reader at excitation/emission wavelengths of 488/525 nm.

Quantitative real-time PCR

After the indicated treatments, total RNA was extracted from HK-2 cells using TRIzol reagent, and RNA concentration and purity were determined. Equal amounts of RNA were reverse-transcribed into cDNA. qPCR was performed using SYBR Green chemistry under the following conditions: initial denaturation at 95°C for 30 s, followed by 40 cycles of 95°C for 5 s and 60°C for 30 s, after which melting-curve analysis was performed. The mRNA expression levels of GDF15, GPX4, SLC7A11, FTH1, TFRC, HAMP, TNF-α, IL-6, IL-1β, and NFKB1 were measured, with β-actin as the internal reference. Relative expression was calculated using the $2^{-}\Delta\Delta Ct$ method. Each sample was analyzed in three technical replicates, and experiments were independently repeated three times. Primer sequences are shown in Supplementary Table 2.

Western blot analysis

After treatment, total protein was extracted from cells using RIPA lysis buffer supplemented with protease and phosphatase inhibitors, and protein concentrations were determined using the BCA assay. Equal amounts of protein were separated by SDS-PAGE and transferred to PVDF membranes. Membranes were blocked for 1 h and incubated overnight at 4°C with primary antibodies against GDF15, GPX4, SLC7A11, ACSL4, p-NF-κB p65, NF-κB p65, and β-actin, followed by incubation with HRP-conjugated secondary antibodies for 1 h at room temperature. Protein bands were visualized using enhanced chemiluminescence, and densitometric analysis was performed with ImageJ. GDF15, GPX4, SLC7A11, and ACSL4 were normalized to β-actin, whereas p-NF-κB p65 was normalized to total NF-κB p65. Experiments were independently repeated three times.

Statistical analysis

Statistical analyses were performed using SPSS version 25.0 and GraphPad Prism version 9.5. Continuous variables were first assessed for normality and homogeneity of variance. Normally distributed data are presented as mean ± standard deviation and were compared among multiple groups using one-way analysis of variance followed by Tukey's post hoc test. Non-normally distributed data are presented as median (interquartile range) and were analyzed using the Kruskal-Wallis test followed by Dunn's multiple-comparison test. Categorical variables are presented as number (percentage) and were compared using the χ^2 test or Fisher's exact test, as appropriate. Correlations between GDF15 and clinical variables were assessed using Spearman rank correlation and are reported as Spearman's ρ. Cell experiments were independently repeated at least three times. All tests were two-sided, and $P<0.05$ was considered statistically significant.

Results

Clinical characteristics and associations of GDF15 with renal injury, ferroptosis-related, and inflammatory markers

Sex distribution and age did not differ significantly among the three groups (all $P>0.05$). Compared with the NC group, both the T2DM and DKD groups had higher BMI, HbA1c, and GLU levels, with BMI and HbA1c further increased in the DKD group (all $P<0.001$). Urea, Cr, and UACR were markedly increased, whereas eGFR was significantly reduced in the DKD group; Urea, Cr, and UACR showed a progressive increase across the three groups (all $P<0.001$). TG was higher in the DKD group than in the NC and T2DM groups, whereas LDL-C was lower in both the T2DM and DKD groups than in the NC group. No significant between-group differences were observed in TC, HDL-C, or AST/ALT (all $P>0.05$) (Table 1).

Table 1. Comparison of baseline clinical characteristics among the study groups

Variable	NC (n=43)	T2DM (n=40)	DKD (n=38)	P value
Sex, male	22 (51.2%)	20 (50.0%)	21 (55.3%)	0.888
Age (years)	52.56 ± 9.66[a]	53.15 ± 11.05[a]	54.32 ± 12.20[a]	0.767
BMI (kg/m²)	22.32 ± 1.37[a]	26.12 ± 1.64[b]	28.87 ± 2.78[c]	<0.001
HbA1c (%)	4.70 ± 0.61[a]	6.90 ± 1.66[b]	9.36 ± 1.09[c]	<0.001
GLU (mmol/L)	5.42 ± 0.39[a]	7.17 ± 1.55[b]	7.95 ± 1.99[b]	<0.001
Urea (mmol/L)	4.74 ± 0.79[a]	5.29 ± 1.10[b]	8.40 ± 2.02[c]	<0.001
Cr (μmol/L)	72.90± 14.14[a]	84.80 ± 14.48[b]	106.12± 17.00[c]	<0.001
eGFR [mL/min/1.73 m²]	100.88±13.40[a]	101.29±14.60[a]	76.22 ± 12.44[b]	<0.001
UACR (mg/g)	4.24 ± 2.60[a]	10.59 ± 3.37[b]	565.46 ± 227.48[c]	<0.001
TC (mmol/L)	4.24 ± 1.01[a]	4.70 ± 1.19[a]	4.45 ± 1.31[a]	0.212
TG (mmol/L)	1.45 ± 0.32[a]	1.56 ± 0.67[a]	2.76 ± 0.70[b]	<0.001
HDL-C (mmol/L)	1.27 ± 0.18[a]	1.22 ± 0.26[a]	1.17 ± 0.32[a]	0.181
LDL-C (mmol/L)	2.72 ± 0.59[a]	2.30 ± 0.60[b]	2.21 ± 0.85[b]	0.002
AST/ALT	0.91 ± 0.31[a]	0.86 ± 0.23[a]	1.00 ± 0.35[a]	0.113

Note: Different superscript letters indicate significant pairwise differences in post hoc comparisons ($P<0.05$); identical letters indicate no significant difference.

Overall differences in GDF15, iron-metabolism parameters, ferroptosis-related antioxidant markers, and inflammatory factors were significant among the three groups (all $P<0.001$). With

respect to iron metabolism, serum Fe was significantly lower in the DKD group, whereas FER increased and TRF decreased progressively across the groups. Consistent with increasing disease severity, GPX4 and GSH decreased from the NC group to the T2DM group and then to the DKD group, whereas GDF15 increased progressively (all P<0.001). The proinflammatory markers IL-1β, IL-17, IL-6, TNF-α, and hs-CRP increased with disease severity. IL-10 was elevated in the T2DM group but reduced in the DKD group (all P<0.001) (Table 2).

Table 2. Comparison of GDF15, iron-metabolism parameters, ferroptosis-related antioxidant markers, and inflammatory factors

Variable	NC (n=43)	T2DM (n=40)	DKD (n=38)	P value
Fe (μmol/L)	18.20 ± 6.06[a]	15.79 ± 4.16[a]	11.82 ± 2.61[b]	<0.001
FER (ng/mL)	112.82 ± 21.52[a]	182.58 ± 77.17[b]	248.67 ± 69.14[c]	<0.001
TRF (g/L)	2.56 ± 0.29[a]	1.97 ± 0.37[b]	1.49 ± 0.27[c]	<0.001
GPX4 (ng/mL)	176.95 ± 31.96[a]	145.81 ± 26.82[b]	102.07 ± 31.49[c]	<0.001
GDF15 (ng/L)	602.00 ± 135.19[a]	1324.68 ± 321.10[b]	1906.65 ± 351.79[c]	<0.001
GSH (μmol/L)	5.54 ± 1.31[a]	4.40 ± 1.52[b]	2.90 ± 0.96[c]	<0.001
IL-1β (pg/mL)	1.51 ± 0.87[a]	2.64 ± 0.88[b]	4.80 ± 2.18[c]	<0.001
IL-17 (pg/mL)	2.50 ± 0.63[a]	4.52 ± 2.77[b]	10.48 ± 6.05[c]	<0.001
IL-10 (pg/mL)	3.65 ± 0.62[a]	5.55 ± 0.43[b]	2.70 ± 0.66[c]	<0.001
IL-6 (pg/mL)	1.71 ± 0.49[a]	4.57 ± 0.96[b]	8.18 ± 1.66[c]	<0.001
TNF-α (pg/mL)	2.15 ± 0.44[a]	9.52 ± 3.37[b]	13.14 ± 3.68[c]	<0.001
hs-CRP (mg/L)	0.82 ± 0.27[a]	2.87 ± 0.62[b]	6.77 ± 1.10[c]	<0.001

Note: Different superscript letters indicate significant pairwise differences in post hoc comparisons (P<0.05); identical letters indicate no significant difference.

Spearman correlation analysis showed that GDF15 was positively correlated with BMI, HbA1c, GLU, Urea, Cr, and UACR and negatively correlated with eGFR (all P<0.001), with a particularly strong correlation with UACR (ρ=0.804). Among iron-metabolism and ferroptosis-related markers, GDF15 was positively correlated with FER and negatively correlated with Fe, TRF, GPX4, and GSH (all P<0.001); the negative correlations with TRF and GPX4 were relatively strong (ρ=−0.722 and −0.646, respectively). Regarding inflammatory markers, GDF15 was positively correlated with IL-1β, IL-17, IL-6, TNF-α, and hs-CRP (all P<0.001), with the strongest correlations observed for IL-6 and hs-CRP (ρ=0.812 and 0.811, respectively). No significant correlation was observed between GDF15 and IL-10 (P=0.135) (Table 3). Correlation heatmaps further illustrated the relationships of GDF15 with renal injury, iron metabolism/ferroptosis, and inflammatory markers (Figure 1A-C).

Table 3. Correlations between GDF15 and clinical variables

Variable	**Age**	**BMI**	**HbA1c**	**GLU**	**Urea**	**Cr**	**eGFR**	**UACR**
ρ	0.110	0.736	0.741	0.525	0.595	0.540	-0.470	0.804
P value	0.228	<0.001	<0.001	<0.001	<0.001	<0.001	<0.001	<0.001
Variable	**TC**	**TG**	**HDL-C**	**LDL-C**	**AST/ALT**	**Fe**	**FER**	**TRF**
ρ	0.051	0.505	-0.056	-0.261	0.079	-0.418	0.637	-0.722
P	0.576	<0.001	0.540	0.004	0.387	<0.001	<0.001	<0.001

Variable	GPX4	IL-1β	IL-17	IL-10	GSH	IL-6	TNF-α	hs-CRP
ρ	-0.646	0.617	0.478	-0.137	-0.557	0.812	0.733	0.811
P value	<0.001	<0.001	<0.001	0.135	<0.001	<0.001	<0.001	<0.001

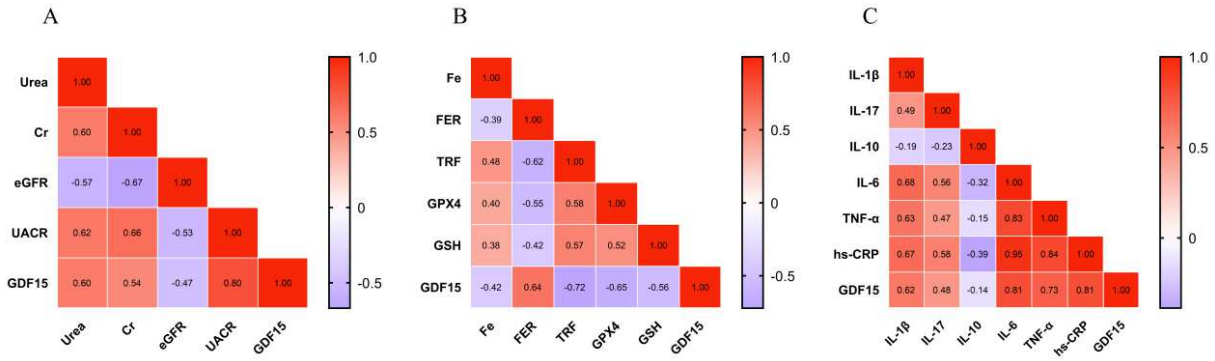


Figure 1. Correlation heatmaps of GDF15 with renal function, iron metabolism/ferroptosis, and inflammatory markers. (A) Renal function-related variables. (B) Iron metabolism- and ferroptosis-related variables. (C) Inflammatory variables. Colors indicate the direction and magnitude of the correlation coefficients.

Taken together, the clinical findings showed that circulating GDF15 was elevated in DKD and was associated with renal dysfunction, altered systemic iron-related indices, reduced circulating antioxidant markers, and inflammation. However, these cross-sectional associations do not establish whether GDF15 contributes to injury or represents a response to metabolic and renal stress. Because serum biomarkers cannot directly establish tubular ferroptosis, we next used HGPA-treated HK-2 cells to investigate the effects of GDF15 modulation on ferroptosis-associated oxidative injury, iron-related gene expression, and inflammatory responses.

Optimization of HGPA modeling conditions and Fer-1 concentration

CCK-8 assays showed that BSA had no significant effect on HK-2 cell viability (P>0.05). Under high-glucose conditions, PA reduced cell viability in a concentration- and time-dependent manner. After treatment with 0.2 mmol/L PA for 24 h, cell viability decreased to approximately 75% of that in the NG group (P<0.0001) without causing excessive cell loss. Therefore, 30 mmol/L glucose combined with 0.2 mmol/L PA for 24 h was selected to establish the HGPA model. DMSO had no significant effect on the viability of HGPA-treated cells (P>0.05), whereas 1 μmol/L Fer-1 produced the greatest improvement in cell viability (P<0.001) and was therefore used in subsequent experiments (Figure 2A-C).

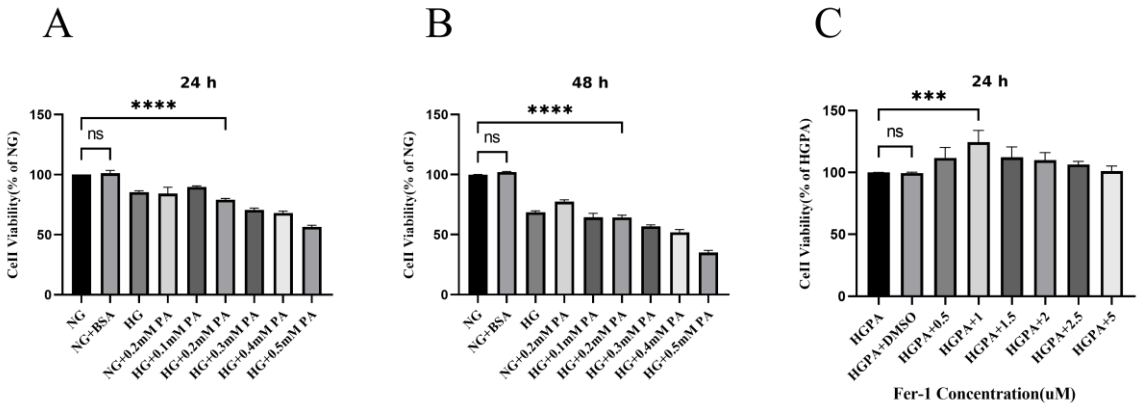


Figure 2. Optimization of HGPA modeling conditions and Fer-1 concentration. (A, B) HK-2 cell viability after treatment with different concentrations of PA for 24 or 48 h. (C) Effects of different concentrations of Fer-1 on the viability of HGPA-treated HK-2 cells. ns, P>0.05; ***P<0.001; ****P<0.0001.

HGPA induces ferroptosis-related injury, iron-homeostasis disturbance, and inflammation in HK-2 cells, accompanied by GDF15 upregulation

To evaluate the effect of HGPA on ferroptosis in HK-2 cells, oxidative-stress and ferroptosis-related biochemical markers were first examined. Compared with the NG group, HGPA

significantly increased intracellular MDA, Fe^{2+}, and ROS levels while reducing GSH content (all $P<0.001$). Fer-1 treatment markedly reduced MDA, Fe^{2+}, and ROS and significantly restored GSH levels (all $P<0.01$), indicating that HGPA induced iron-dependent oxidative injury in HK-2 cells and that this process was partially reversed by Fer-1 (Figure 3A-D).

qRT-PCR and Western blot analyses showed that HGPA increased GDF15 expression, decreased GPX4 and SLC7A11 expression, and increased ACSL4 protein abundance; these changes were partially reversed by Fer-1 (Figure 3E, G-K). These findings support the notion that HGPA disrupts the system Xc−/GSH/GPX4 antioxidant defense axis, promotes iron-dependent oxidative injury, and concurrently induces GDF15 expression.

Analysis of iron-metabolism-related genes showed that HGPA decreased FTH1 mRNA while increasing TFRC and HAMP mRNA; Fer-1 partially reversed these changes (all $P<0.05$; Figure 3F), indicating altered expression of genes involved in iron storage, uptake, and regulation. HGPA also increased TNF-α, IL-6, IL-1β, and NFKB1 mRNA levels and elevated the p-NF-κB p65/NF-κB p65 ratio, whereas these inflammatory indices were reduced after Fer-1 treatment (Figure 3L-N). Collectively, HGPA induced ferroptosis-related injury, disturbed iron homeostasis, and activated NF-κB-associated inflammatory responses in HK-2 cells, accompanied by increased GDF15 expression; Fer-1 partially alleviated these changes.

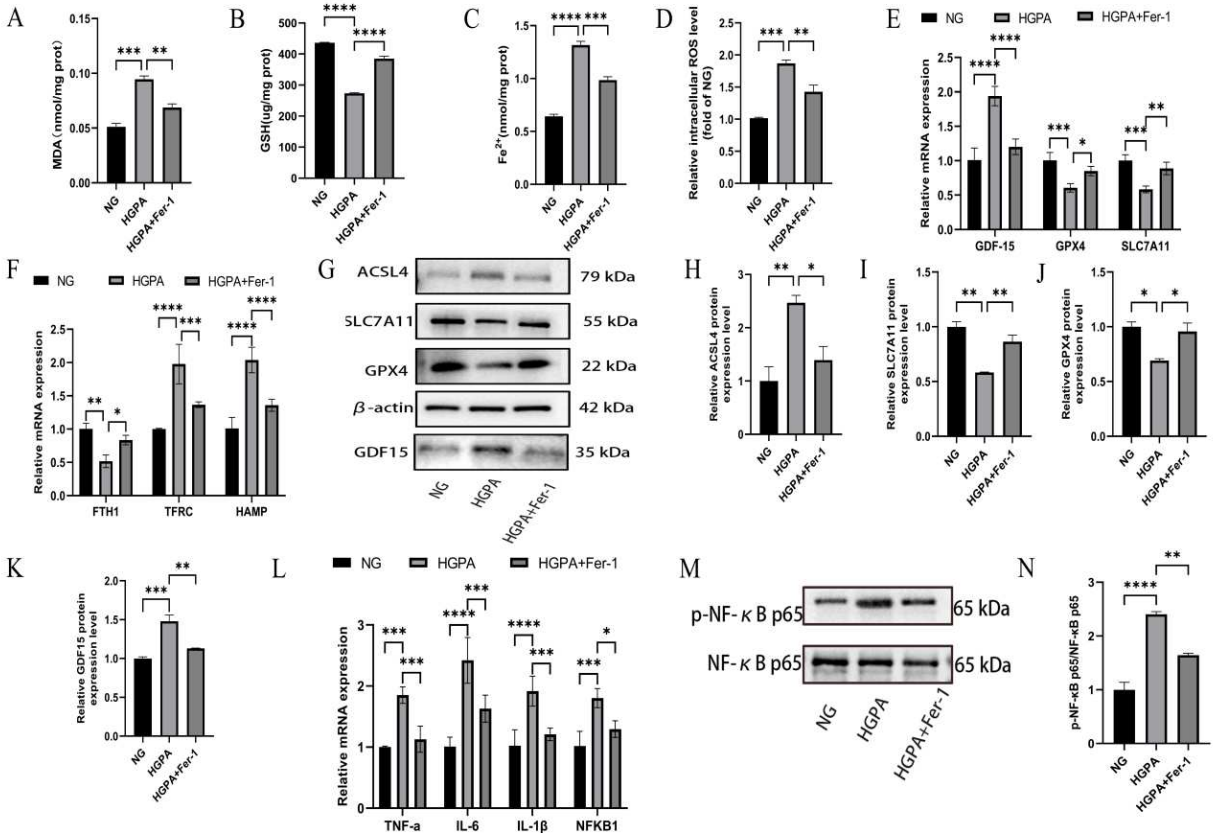


Figure 3. HGPA induces ferroptosis-related injury, dysregulation of iron-metabolism genes, and inflammatory responses in HK-2 cells, accompanied by GDF15 upregulation. HK-2 cells were assigned to the NG, HGPA, and HGPA+Fer-1 groups. (A-D) Cellular MDA, GSH, Fe^{2+}, and ROS, respectively. (E) mRNA expression of GDF15, GPX4, and SLC7A11. (F) mRNA expression of FTH1, TFRC, and HAMP. (G) Representative Western blots of GDF15, ACSL4, SLC7A11, and GPX4. (H-K) Densitometric quantification of the corresponding proteins. (L) mRNA expression of TNF-α, IL-6, IL-1β, and NFKB1. (M, N) Representative blots of p-NF-κB p65 and NF-κB p65 and the corresponding ratio. Data are presented as mean ± SD from three independent experiments. *P<0.05, **P<0.01, ***P<0.001, ****P<0.0001.

GDF15 knockdown aggravates HGPA-induced ferroptosis-related injury, iron-homeostasis imbalance, and inflammation

The knockdown efficiencies of three GDF15-targeting siRNAs were evaluated under HGPA

conditions. siGDF15-1 produced the greatest reduction in GDF15 mRNA and protein expression and was therefore selected for subsequent experiments (Figure 4).

Compared with HGPA+siNC, GDF15 knockdown increased MDA, Fe^{2+}, and ROS levels and reduced GSH, together with lower GPX4 and SLC7A11 expression and higher ACSL4 protein abundance (Figure 5A–K). The knockdown group also showed reduced FTH1 and increased TFRC and HAMP transcripts, along with elevated inflammatory gene expression and a higher p-p65/total p65 ratio (Figure 5F, L–N). Fer-1 partially mitigated these alterations without materially restoring GDF15 expression. Together, these observations suggest that endogenous GDF15 limits HGPA-induced injury and that ferroptosis-related processes contribute to the enhanced injury phenotype observed after GDF15 knockdown.

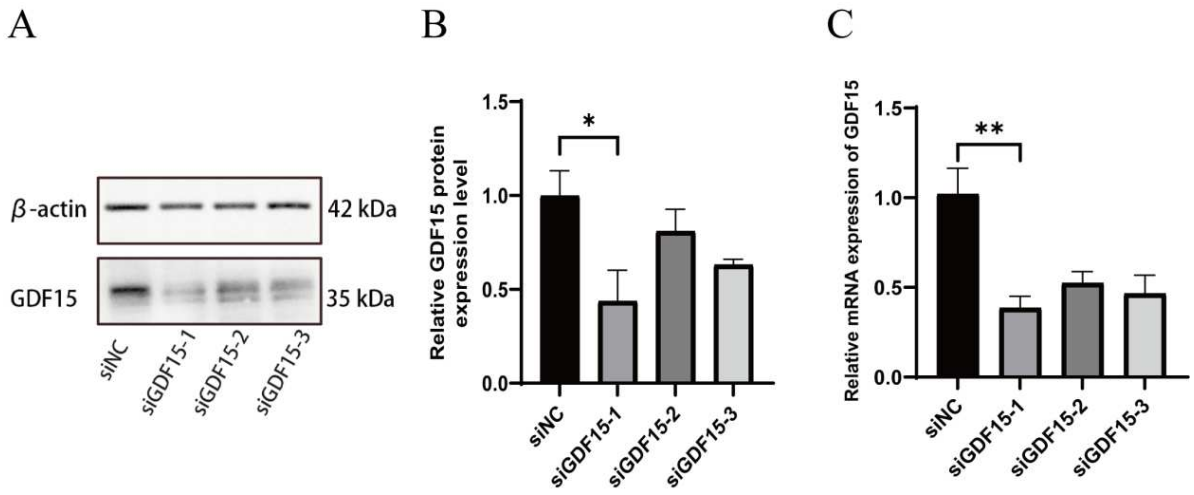


Figure 4. Screening of GDF15-targeting siRNA sequences. (A) Representative Western blots of GDF15 protein after transfection with siNC, siGDF15-1, siGDF15-2, or siGDF15-3. (B) Densitometric quantification of GDF15 protein. (C) GDF15 mRNA expression. All groups were exposed to identical HGPA treatment. Protein expression was normalized to β-actin. Data are presented as mean ± SD, n=3. *P<0.05, **P<0.01.

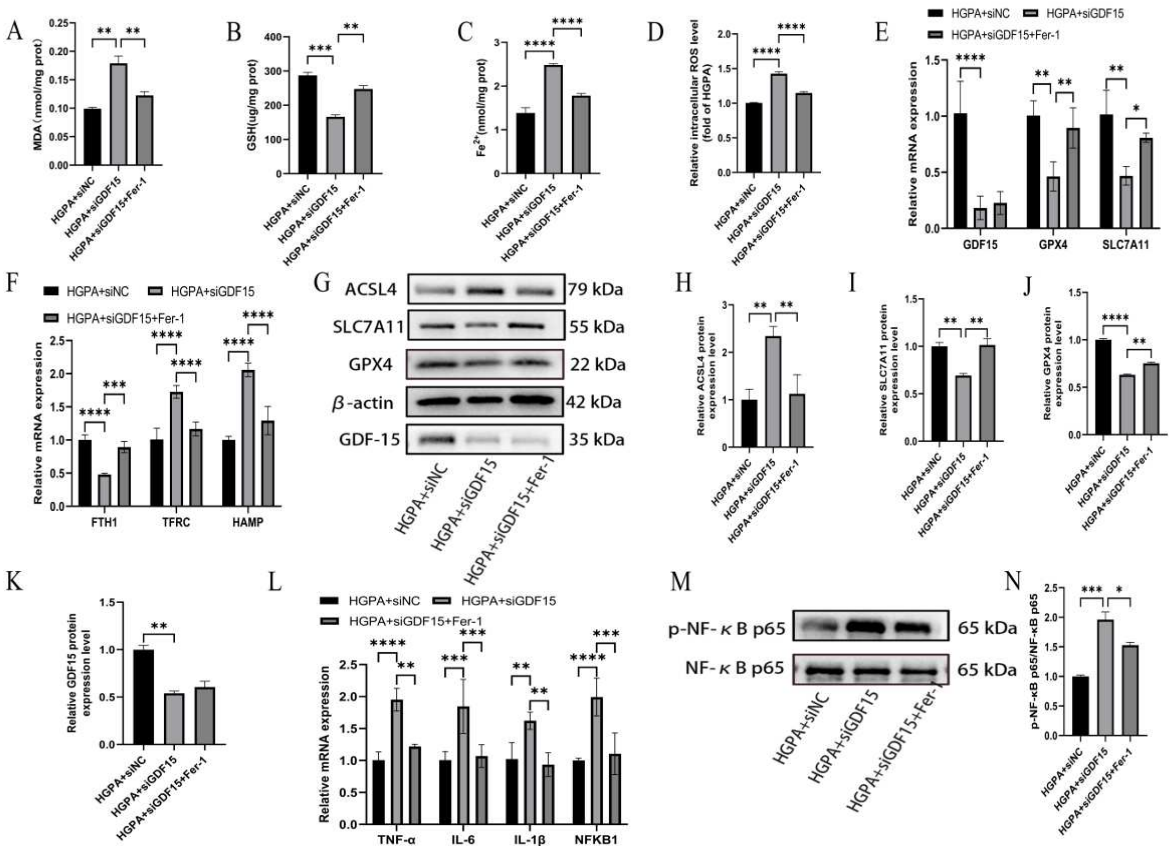


Figure 5. GDF15 knockdown aggravates HGPA-induced ferroptosis, iron-homeostasis imbalance, and inflammation in HK-2 cells, which are partially reversed by Fer-1. HK-2 cells were assigned to the HGPA+siNC, HGPA+siGDF15, and HGPA+siGDF15+Fer-1 groups. (A-D) Intracellular MDA, GSH, Fe^{2+}, and ROS, respectively. (E) mRNA expression of GDF15, GPX4, and SLC7A11. (F) mRNA expression of FTH1, TFRC, and HAMP. (G) Representative Western blots of GDF15, GPX4, SLC7A11, and ACSL4. (H-K) Densitometric quantification of the corresponding proteins. (L) mRNA expression of TNF-α, IL-6, IL-1β, and NFKB1. (M, N) Representative blots of p-NF-κB p65 and NF-κB p65 and the corresponding ratio. Data are presented as mean ± SD, n=3. *P<0.05, **P<0.01, ***P<0.001, ****P<0.0001.

GDF15 overexpression attenuates HGPA-induced ferroptosis-related injury, iron-metabolism abnormalities, and inflammation

To investigate the regulatory effect of GDF15 on HGPA-induced HK-2 cell injury, cells were

transfected with a GDF15 overexpression plasmid under HGPA conditions. Compared with the HGPA+Vector group, GDF15 mRNA and protein expression were increased in the HGPA+OE-GDF15 group, confirming successful establishment of the GDF15 overexpression model. GDF15 overexpression decreased MDA, Fe^{2+}, and ROS levels and increased GSH, while upregulating GPX4 and SLC7A11 and downregulating ACSL4. Co-treatment with Fer-1 shifted these indices further toward a protective profile (Figure 6A-G, I-L). These results indicate that GDF15 overexpression attenuates HGPA-induced oxidative injury, lipid peroxidation, and ferroptosis-related phenotypes.

GDF15 overexpression also increased FTH1 mRNA, decreased TFRC and HAMP mRNA, and reduced intracellular Fe^{2+}, suggesting a potential role in maintaining cellular iron homeostasis. With respect to inflammation, GDF15 overexpression reduced TNF-α, IL-6, IL-1β, and NFKB1 mRNA expression and decreased the p-NF-κB p65/NF-κB p65 ratio; these indices were further reduced after combined Fer-1 treatment (Figure 6H, M-O). These findings support the ability of GDF15 to simultaneously attenuate HGPA-induced ferroptosis-related injury and NF-κB-associated inflammation, although they do not establish NF-κB as a direct downstream pathway through which GDF15 regulates ferroptosis.

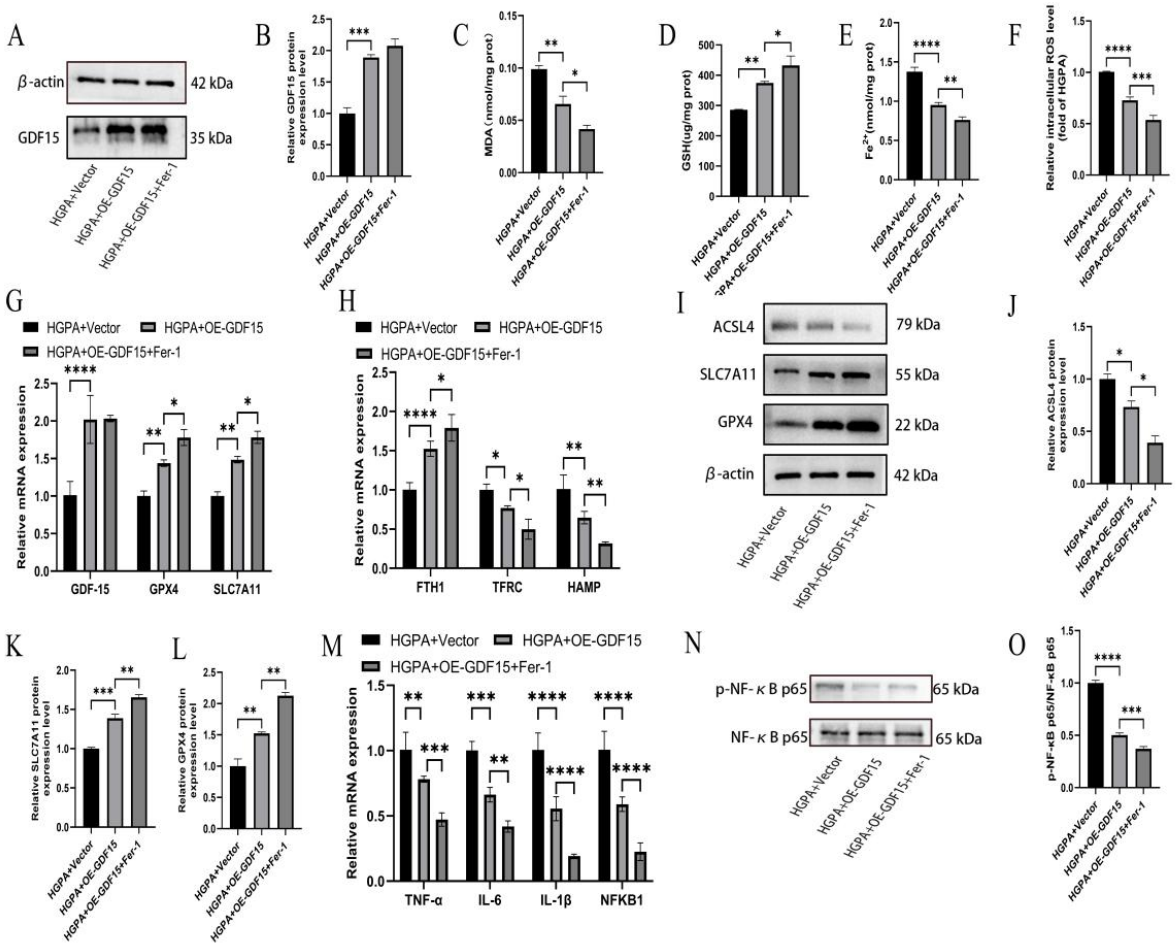


Figure 6. GDF15 overexpression attenuates HGPA-induced ferroptosis-related injury, iron-metabolism abnormalities, and inflammatory responses. HK-2 cells were assigned to the HGPA+Vector, HGPA+OE-GDF15, and HGPA+OE-GDF15+Fer-1 groups. (A, B) Validation of GDF15 overexpression. (C-F) MDA, GSH, Fe^{2+}, and ROS. (G) mRNA expression of GDF15, GPX4, and SLC7A11. (H) mRNA expression of FTH1, TFRC, and HAMP. (I-L) Representative Western blots and densitometric quantification of ACSL4, SLC7A11, and GPX4. (M) mRNA expression of TNF-α, IL-6, IL-1β, and NFKB1. (N, O) Representative blots of p-NF-κB p65 and NF-κB p65 and the corresponding ratio. Data are presented as mean ± SD, n=3. *P<0.05, **P<0.01, ***P<0.001, ****P<0.0001.

Discussion

In addition to confirming the presence of ferroptosis-related alterations and elevated GDF15 levels in DKD, the present study integrated clinical phenotypes, glucolipotoxic stress, cellular iron homeostasis, and inflammatory signaling into a coherent framework. Previous studies have independently demonstrated that GDF15 is associated with DKD progression[16] , that GDF15 may alleviate diabetic renal injury, and that renal tubular ferroptosis contributes to DKD [17, 18]. However, these processes have largely been investigated separately. The present study integrated clinical observations with cellular experiments to investigate the potential role of GDF15 in diabetic kidney disease (DKD). We found that circulating GDF15 levels were associated with renal dysfunction, altered systemic iron-related parameters, reduced antioxidant markers, and inflammatory indices in patients with DKD. Furthermore, bidirectional manipulation of GDF15 expression in HGPA-treated HK-2 cells revealed corresponding changes in ferroptosis-associated oxidative injury, iron-metabolism-related gene expression, and NF-κB-associated inflammatory responses. By combining clinical associations with functional cellular observations, our findings provide additional evidence linking GDF15 to glucolipotoxic tubular injury. Nevertheless, the specific molecular pathways underlying these effects remain to be elucidated.

The clinical findings first support the potential of GDF15 as an integrated stress-related biomarker of DKD. Serum GDF15 levels were significantly higher in patients with DKD than in healthy controls and patients with T2DM without DKD. Moreover, GDF15 was positively correlated with UACR, serum urea, and creatinine and negatively correlated with eGFR. These findings are consistent with previous studies showing that GDF15 increases with the severity of albuminuria, correlates positively with creatinine and BUN, and correlates inversely with eGFR [9, 11]. Prospective studies have further demonstrated that elevated baseline GDF15 levels can predict the progression of albuminuria in patients with T2DM [19, 20]. In addition, we observed negative correlations of GDF15

with GPX4, GSH, serum iron, and transferrin, whereas positive correlations were found with ferritin and several pro-inflammatory markers. These associations are broadly consistent with previous population-based observations linking GDF15 to iron metabolism and systemic inflammation [21, 22], thereby providing clinical evidence supporting the biological relevance of GDF15 in DKD.

Nevertheless, these clinical associations should be interpreted cautiously. Circulating GPX4 and GSH primarily reflect systemic antioxidant capacity rather than renal tissue-specific redox status, and their alterations may partly result from systemic oxidative stress or changes in hepatic metabolism rather than tubular ferroptosis per se. Furthermore, the increase in circulating GDF15 accompanying declining eGFR may be partially influenced by reduced renal clearance and consequent GDF15 accumulation. Because the correlation analyses were performed across the three study groups, the observed effect sizes may also have been amplified by between-group gradients in disease severity. Accordingly, these findings should be interpreted as associations across a continuum of disease severity rather than evidence that elevated GDF15 itself is causally responsible for renal injury. The clinical data alone cannot distinguish whether increased GDF15 represents a marker of tissue damage, a consequence of impaired renal clearance, or an adaptive response to cellular stress. This uncertainty provided the rationale for subsequent functional validation at the cellular level.

To further clarify the role of GDF15 in the diabetic renal environment while minimizing the influence of systemic confounders, HK-2 cells were exposed to high glucose combined with palmitic acid to mimic the hyperglycemic and lipid-overload conditions characteristic of DKD. Bidirectional manipulation of GDF15 expression together with Fer-1 rescue experiments was then used to evaluate the effects of GDF15 on glucolipotoxicity-induced ferroptosis, iron dyshomeostasis, and inflammatory responses in renal tubular epithelial cells. HGPA treatment decreased cell viability and

increased ROS, MDA, and Fe^{2+} levels while reducing intracellular GSH. These changes were accompanied by downregulation of GPX4 and SLC7A11 and upregulation of ACSL4, supporting disruption of the System Xc^-/GSH/GPX4 antioxidant axis, iron-dependent lipid peroxidation, and ACSL4-mediated activation of polyunsaturated fatty acids as key features of ferroptosis [23-26]. In particular, ACSL4 facilitates the incorporation of polyunsaturated fatty acids into membrane phospholipids, thereby increasing the availability of substrates susceptible to lipid peroxidation [27]. Importantly, Fer-1 partially reversed these alterations, further supporting a substantial contribution of iron-dependent lipid peroxidation to HGPA-induced cellular injury.

Notably, HGPA-induced ferroptotic injury was also accompanied by marked alterations in iron-regulatory genes, including increased TFRC and decreased FTH1 mRNA expression [28]. Such transcriptional reprogramming may favor increased cellular iron uptake while reducing intracellular iron-storage capacity, thereby expanding the labile iron pool and providing additional catalytic iron for Fenton chemistry. In parallel, increased HAMP expression may represent an adaptive attempt to regulate iron availability by restricting iron export; however, under glucolipotoxic conditions, such a response may instead promote intracellular iron retention and contribute to iron overload [29].

Altered iron homeostasis may therefore represent an important mechanistic link between GDF15 and lipid peroxidation. Both HGPA exposure and GDF15 knockdown were associated with decreased FTH1 expression, increased TFRC and HAMP expression, and intracellular Fe^{2+} accumulation, whereas GDF15 overexpression shifted these parameters in the opposite direction. Reduced FTH1 may impair the cellular capacity to safely sequester redox-active iron, whereas increased TFRC may enhance iron uptake. In addition, NCOA4-mediated ferritinophagy can promote the release of free iron through ferritin degradation, thereby modulating cellular

susceptibility to ferroptosis [30, 31]. Previous studies in patients with diabetes have also suggested associations among GDF15, renal function, and iron-regulatory parameters, although the relationships between GDF15 and individual iron indices appear to vary across different stages of disease [32, 33]. HGPA also markedly increased the p-p65/p65 ratio and enhanced the transcription of pro-inflammatory mediators, including TNF-α, IL-6, and IL-1β. IL-6 is known to induce HAMP expression, while hepcidin limits cellular iron export by promoting ferroportin degradation, contributing to inflammation-associated hypoferremia and potentially enhancing intracellular iron retention [34, 35]. These findings suggest that ferroptosis and inflammation may interact to amplify tubular epithelial injury, providing several potential points at which GDF15 may exert protective effects.

The bidirectional manipulation of GDF15 together with Fer-1 rescue experiments provided the principal functional evidence supporting a protective role of GDF15 in the present study. Under HGPA conditions, GDF15 knockdown further suppressed GPX4 and SLC7A11 expression and increased ACSL4 expression, accompanied by greater accumulation of Fe^{2+}, MDA, and ROS and more pronounced GSH depletion. In contrast, GDF15 overexpression substantially reversed these ferroptosis-associated changes, restored FTH1 expression, and reduced TFRC and HAMP transcription. Importantly, Fer-1 attenuated the downstream injury caused by GDF15 knockdown without restoring GDF15 expression itself, suggesting that ferroptosis-related processes constitute an important component of the phenotype resulting from GDF15 deficiency. Previous studies have shown that GDF15 expression is increased in diabetic renal tissue and in podocytes exposed to high glucose. GDF15 knockdown aggravated inflammation and podocyte injury, whereas GDF15 overexpression suppressed inflammatory responses through modulation of the NEDD4L–IKK/IκBα–NF-κB signaling axis, suggesting that increased GDF15 may serve as an endogenous

protective response in DKD [18]. More recently, studies of acute kidney injury have demonstrated that GDF15 intervention simultaneously improves GSH, GPX4, SLC7A11, Fe^{2+}, and MDA abnormalities in HK-2 cells while suppressing TLR4/MyD88/NF-κB signaling [36]. These findings further support the biological plausibility of an anti-ferroptotic role for GDF15, whereas the present study extends this protective effect specifically to the glucolipotoxic environment relevant to DKD.

The interplay between ferroptosis and inflammatory signaling represents another important finding of this study. Both HGPA exposure and GDF15 knockdown increased the expression of TNF-α, IL-6, IL-1β, and NFKB1 and enhanced the p-NF-κB p65/NF-κB p65 ratio, whereas both Fer-1 treatment and GDF15 overexpression attenuated these alterations. NF-κB is a central transcriptional regulator integrating oxidative stress and innate immune signaling and controls the expression of numerous pro-inflammatory mediators [37, 38]. These observations are consistent with our findings and suggest that GDF15 may attenuate NF-κB-mediated inflammatory amplification, potentially in part by limiting labile iron accumulation and lipid peroxidation. Collectively, the data indicate that GDF15 influences both redox homeostasis and inflammatory signaling and raise the possibility of reciprocal crosstalk between ferroptotic stress and NF-κB activation. However, the present experiments do not establish NF-κB as a direct downstream mediator of the anti-ferroptotic effects of GDF15.

Several limitations of this study should be acknowledged. First, the clinical component was conducted at a single center with a relatively limited sample size, precluding conclusions regarding the temporal or causal relationship between GDF15 and DKD progression. Potential confounding factors, including age, renal clearance, and pharmacological treatment, were also not fully addressed using multivariable models. Second, circulating GPX4, GSH, and iron-related indices reflect

systemic alterations and cannot be considered direct evidence of ferroptosis within renal tissue. Third, although the cellular experiments established a functional sequence using GDF15 knockdown, overexpression, and Fer-1 rescue, lipid ROS measured using C11-BODIPY, mitochondrial ultrastructural alterations, and a second ferroptosis inhibitor were not assessed. Furthermore, FTH1, TFRC, and HAMP were evaluated only at the mRNA level, and specific pharmacological inhibition or activation of NF-κB was not performed. Future studies incorporating animal models, renal tissue validation, and prospective clinical cohorts, together with pathway-specific rescue experiments, are therefore warranted to define the causal hierarchy among GDF15, iron homeostasis, ferroptosis, and NF-κB signaling.

Conclusion

This study demonstrates that elevated serum GDF15 levels are associated with markers of renal injury and that GDF15 exerts protective effects in HK-2 cells exposed to glucolipotoxic stress. These effects may involve increased GSH levels, upregulation of GPX4 and SLC7A11, and downregulation of ACSL4, accompanied by attenuation of ferroptosis-associated oxidative injury and inflammatory responses. These findings provide experimental evidence supporting further investigation of GDF15 and its potential therapeutic relevance in diabetic kidney disease.

Author contributions

X.Z. and Y.L. conceived and designed the study. X.Z., H.B., K.Z., Z.W., J.D., X.Y. and J.N. contributed to clinical sample collection, laboratory experiments and data acquisition. X.Z. performed the statistical analyses, prepared the figures and drafted the manuscript. Y.L. supervised the study and revised the manuscript. All authors reviewed and approved the final version of the manuscript.

Funding

Central Guidance Funds for Local science and technology Development projects（264Z7759G）; Government-funded Project for Cultivating Outstanding Clinical Medical Talents in 2026 (ZF2026022)

Data availability statement

The data supporting the findings of this study are available from the corresponding author upon reasonable request.

Ethics approval and consent to participate

This study was conducted in accordance with the ethical principles of the Declaration of Helsinki and relevant ethical guidelines for biomedical research involving human participants. The study protocol was reviewed and approved by the Ethics Committee of Hebei General Hospital, Shijiazhuang, China (Ethics Approval No. (2025) 598).

Agree and publish

Not Applicable

Conflict of interest

All the authors declare that they have no conflicts of interest related to this study.

Clinical trial number

Not applicable

References

[1] Global, regional, and national burden of chronic kidney disease in adults, 1990-2023, and its attributable risk

factors: a systematic analysis for the Global Burden of Disease Study 2023 [J]. Lancet, 2025, 406(10518): 2461-82.

[2] HU S, HANG X, WEI Y, et al. Crosstalk among podocytes, glomerular endothelial cells and mesangial cells in diabetic kidney disease: an updated review [J]. Cell Commun Signal, 2024, 22(1): 136.

[3] LI M, LI C M, YE Z C, et al. A retrospective cohort study on the pathology and outcomes of type 2 diabetic patients with renal involvement [J]. Int urol nephrol, 2021, 53(2): 333-41.

[4] DIXON S J, LEMBERG K M, LAMPRECHT M R, et al. Ferroptosis: an iron-dependent form of nonapoptotic cell death [J]. Cell, 2012, 149(5): 1060-72.

[5] KIM S, KANG S W, JOO J, et al. Characterization of ferroptosis in kidney tubular cell death under diabetic conditions [J]. Cell Death Dis, 2021, 12(2): 160.

[6] WANG Y, BI R, QUAN F, et al. Ferroptosis involves in renal tubular cell death in diabetic nephropathy [J]. Eur j pharmacol, 2020, 888(-): 173574.

[7] LU Q, YANG L, XIAO J J, et al. Empagliflozin attenuates the renal tubular ferroptosis in diabetic kidney disease through AMPK/NRF2 pathway [J]. Free radical bio med, 2023, 195(-): 89-102.

[8] WANG Y H, CHANG D Y, ZHAO M H, et al. Dapagliflozin Alleviates Diabetic Kidney Disease via Hypoxia Inducible Factor 1α/Heme Oxygenase 1-Mediated Ferroptosis [J]. Antioxid redox sign, 2024, 40(7-9): 492-509.

[9] CARLSSON A C, NOWAK C, LIND L, et al. Growth differentiation factor 15 (GDF-15) is a potential biomarker of both diabetic kidney disease and future cardiovascular events in cohorts of individuals with type 2 diabetes: a proteomics approach [J]. Upsala j med sci, 2020, 125(1): 37-43.

[10] HO J E, HWANG S J, WOLLERT K C, et al. Biomarkers of cardiovascular stress and incident chronic kidney disease [J]. Clin chem, 2013, 59(11): 1613-20.

[11] OSHITA T, WATANABE S, TOYOHARA T, et al. Urinary growth differentiation factor 15 predicts renal function decline in diabetic kidney disease [J]. Sci Rep, 2023, 13(1): 12508.

[12] MAZAGOVA M, BUIKEMA H, VAN BUITEN A, et al. Genetic deletion of growth differentiation factor 15 augments renal damage in both type 1 and type 2 models of diabetes [J]. Am j physiol-renal, 2013, 305(9): F1249-64.

[13] CHEN J, PENG H, CHEN C, et al. NAG-1/GDF15 inhibits diabetic nephropathy via inhibiting AGE/RAGE-mediated inflammation signaling pathways in C57BL/6 mice and HK-2 cells [J]. Life sci, 2022, 311(Pt A): 121142.

[14] VALIñO-RIVAS L, CUARENTAL L, CEBALLOS M I, et al. Growth differentiation factor-15 preserves Klotho expression in acute kidney injury and kidney fibrosis [J]. Kidney int, 2022, 101(6): 1200-15.

[15] XIA M, ZHANG Q, ZHANG Y, et al. Growth Differentiation Factor 15 Regulates Oxidative Stress-Dependent Ferroptosis Post Spinal Cord Injury by Stabilizing the p62-Keap1-Nrf2 Signaling Pathway [J]. Front aging neurosci, 2022, 14(-): 905115.

[16] HUANG X, YU N, YU H, et al. Association of growth differentiation factor-15 with renal disease outcomes and all-cause death in type 1 and type 2 diabetic patients: a meta-analysis [J]. Bmc nephrol, 2025, 27(1): 8.

[17] CHEN J, LIU D, LEI L, et al. CNPY2 Aggravates Renal Tubular Cell Ferroptosis in Diabetic Nephropathy by Regulating PERK/ATF4/CHAC1 Pathway and MAM Integrity [J]. Adv sci, 2025, -(-): e2416441.

[18] ZHANG X, WANG S, CHONG N, et al. GDF-15 alleviates diabetic nephropathy via inhibiting NEDD4L-mediated IKK/NF-κB signalling pathways [J]. Int immunopharmacol, 2024, 128(-): 111427.

[19] CHUNG J O, CHUNG M Y, PARK S Y, et al. Relationship between plasma growth differentiation factor-15 level and estimated glomerular filtration rate in type 2 diabetes patients with and without albuminuria [J]. J diabetes complicat, 2021, 35(4): 107849.

[20] HELLEMONS M E, MAZAGOVA M, GANSEVOORT R T, et al. Growth-differentiation factor 15 predicts worsening of albuminuria in patients with type 2 diabetes [J]. Diabetes care, 2012, 35(11): 2340-6.

[21] TAJES M, RAS-JIMéNEZ M D M, GIRONA J, et al. Serum Growth Differentiation Factor 15 (GDF15) Levels

Reflect Ischemic Etiology in Heart Failure Patients with Iron Deficiency: A Cross-Sectional Study [J]. Biomolecules, 2025, 15(9): -.

[22] YILMAZ A, KAYMAZ T, YAKAR B, et al. Serum levels of GDF-15, betatrophin, TNF-α and IL-6 in diabetic patients with and without diabetic complications [J]. Saudi Med J, 2025, 46(9): 1033-8.

[23] BERNDT C, ALBORZINIA H, AMEN V S, et al. Ferroptosis in health and disease [J]. Redox biol, 2024, 75(-): 103211.

[24] DOLL S, PRONETH B, TYURINA Y Y, et al. ACSL4 dictates ferroptosis sensitivity by shaping cellular lipid composition [J]. Nat chem biol, 2017, 13(1): 91-8.

[25] MISHIMA E, NAKAMURA T, DOLL S, et al. Recommendations for robust and reproducible research on ferroptosis [J]. Nat rev mol cell bio, 2025, -(-): -.

[26] ZHENG J, CONRAD M. Ferroptosis: when metabolism meets cell death [J]. Physiol rev, 2025, 105(2): 651-706.

[27] JIANG Y, ZHANG M, SUN M. ACSL4 at the helm of the lipid peroxidation ship: a deep-sea exploration towards ferroptosis [J]. Front pharmacol, 2025, 16(-): 1594419.

[28] WANG H, YU X, LIU D, et al. VDR Activation Attenuates Renal Tubular Epithelial Cell Ferroptosis by Regulating Nrf2/HO-1 Signaling Pathway in Diabetic Nephropathy [J]. Adv sci, 2024, 11(10): e2305563.

[29] WANG J, SHI H, YANG Y, et al. Crosstalk between ferroptosis and innate immune in diabetic kidney disease: mechanisms and therapeutic implications [J]. Front immunol, 2025, 16(-): 1505794.

[30] NING J, WEN L, QIAO L. Ferritinophagy: molecular mechanisms and its crosstalk with ferroptosis in chronic respiratory diseases [J]. Cell biol toxicol, 2026, 42(1): 31.

[31] WANG M, ZHANG Y, CHEN D, et al. NCOA4-Mediated Ferroptosis Drives Tubulointerstitial Fibrosis in Hyperuricemia-Associated Chronic Kidney Disease [J]. Nephrology, 2026, 31(6): e70228.

[32] LUKASZYK E, LUKASZYK M, KOC-ZORAWSKA E, et al. GDF-15, iron, and inflammation in early chronic kidney disease among elderly patients [J]. Int urol nephrol, 2016, 48(6): 839-44.

[33] ZAPORA-KUREL A, KUŹMA Ł, ZAKRZEWSKA M, et al. Novel Iron Parameters in Patients with Type 2 Diabetes Mellitus in Relation to Kidney Function [J]. J Clin Med, 2021, 10(16): -.

[34] GALY B, CONRAD M, MUCKENTHALER M. Mechanisms controlling cellular and systemic iron homeostasis [J]. Nat rev mol cell bio, 2024, 25(2): 133-55.

[35] NEMETH E, RIVERA S, GABAYAN V, et al. IL-6 mediates hypoferremia of inflammation by inducing the synthesis of the iron regulatory hormone hepcidin [J]. J clin invest, 2004, 113(9): 1271-6.

[36] YANG C, ZHAO L, DI J, et al. Growth Differentiation Factor 15 (GDF15) Protects Against Sepsis-Associated Acute Kidney Injury via Suppression of TLR4-MyD88-NF-κB Signaling and Ferroptosis [J]. Biofactors, 2026, 52(4): e70138.

[37] GUO Q, JIN Y, CHEN X, et al. NF-κB in biology and targeted therapy: new insights and translational implications [J]. Signal Transduct Target Ther, 2024, 9(1): 53.

[38] MAO H, ZHAO X, SUN S C. NF-κB in inflammation and cancer [J]. Cell mol immunol, 2025, -(-): -.

Supplementary Files

This is a list of supplementary files associated with this preprint. Click to download.

- Supplementarymaterials.docx
- Uncroppedgelimages20261030170338.pdf